Brief Communication: annual large-scale atmospheric circulation reconstructed from a data assimilation framework cannot explain local East Antarctic ice rises' surface mass balance records

Marie G.P. Cavitte[1], Hugues Goosse[1], Quentin Dalaiden[1], and Nicolas Ghilain[2,3]

[1]Earth and Life Institute (ELI), Université catholique de Louvain-La-Neuve (UCLouvain), Louvain-la-Neuve, Belgium
[2]Royal Meteorological Institute of Belgium, Brussels, Belgium
[3]Département de géographie, Climatologie et Topoclimatologie, Université de Liège

Correspondence: Marie G.P. Cavitte (mariecavitte@gmail.com)

Abstract. Ice cores are influenced by local processes that alter surface mass balance (SMB) records. To evaluate if large-scale atmospheric circulation explains contrasted SMB trends at eight East Antarctic ice rises, we assimilated ice core SMB records within a high-resolution downscaled atmospheric model, while incorporating radar-derived SMB constraints to quantify local observation errors. The reconstruction captures the diverse variability from SMB records but may over-fit by introducing
5   unrealistic wind spatial heterogeneity. While local errors are quantified, they might not cover all uncertainties. Moreover, small-scale wind circulation, unresolved in the reconstruction, could significantly affect local ice core SMB signals.

1   Introduction

Surface mass balance (SMB), which is the net accumulation or removal of snowfall at the surface, over Antarctica is not well
10   understood while it is a very important term for net global sea level rise (Lenaerts et al., 2019). The East Antarctic Ice Sheet, with its high elevation and very cold temperatures has a strong potential to mitigate sea level, with a calculated 0.77 mm of global sea level mitigated over the twentieth century (Medley and Thomas, 2019). However, characterized by high snowfall rates along the coast and low over the plateau, with strong katabatic winds, the East Antarctic Ice Sheet shows strong spatial variability of SMB (Hirsch et al., 2023). Regional climate models with a high spatial resolution (∼a few km^2), such as the
15   polar-oriented Regional Atmospheric Climate Model version 2.3 (RACMO) (Van Wessem et al., 2018), struggle to capture the mean SMB state in the ice sheet interior, while they have a reasonably good fit with coastal mean SMB (e.g. Agosta et al., 2019). However, they lack in spatial variability along the coastline, mostly due to their grid resolution, as shown in Kausch et al. (2020) for the Dronning Maud Land coast.

   To reconstruct SMB beyond direct instrumental measurements, which only cover the last decade or two (Wang et al., 2021),
20   ice cores are the main in-situ observations (Lenaerts et al., 2019). Ice cores provide historical records with a high temporal

resolution, seasonal in the firn and annual down to hundreds of meters. However, ice cores are point measurements with a surface footprint of a few cm^2. These records are therefore influenced by local processes that can lead to different SMB values compared to nearby locations, mainly because of wind erosion and redistribution (Casado et al., 2020). Cavitte et al. (2022) have shown that, in the case of East Antarctic ice rises, this can lead to a systematic underestimation of the SMB on the summit

25 of ice rises as recorded in the ice cores, but that the temporal variability of the SMB is generally well captured.

Data assimilation (DA) allows to optimally combine model simulations and observations to reconstruct past climate variations. DA offers thus the possibility to reconstruct spatial fields from noisy data with sparse spatial coverage and is well adapted to reconstruct SMB from ice core records (Dalaiden et al., 2021). However, DA requires an estimation of the error for any assimilated record. In a DA framework, the observation error dictates the confidence in the climate data in reconstructing

30 variables by dictating the weight of each record in the final reconstruction. The observation error is a combination of two errors: the measurement error - quantified from the published data sets - and the representativeness error - which quantifies what size area an observation is representative of. The representativeness error is difficult to quantify and is traditionally estimated based on prior knowledge or comparing records in a same area such as grid points in model simulations (e.g. Dalaiden et al., 2021; Valler et al., 2020). An innovation in this study is to account for the representativeness error using ice-penetrating radar. With

35 data points every few meters in a radar survey, ice-penetrating radar provides the opportunity to build detailed spatial maps of SMB (e.g. Kausch et al., 2020). By comparing radar-derived SMB and co-located ice cores' measured SMB, we are able to quantify the error of representativeness of the ice core records (Cavitte et al., 2023). This representativeness error can then be directly included in the DA framework that incorporates the local ice core SMB records.

Here, we test if using the representativeness error derived from radar data improves the reconstruction of SMB of the

40 Dronning Maud Land (DML) region over the past 25 years based on the assimilation of eight ice core SMB series by taking advantage of the recent compilation provided in Cavitte et al. (2023). These eight ice core SMB records have an annual resolution with differing trends in close proximity (∼100-300 km between ice rises, Fig. 1a).

Our goal is then to understand whether the contrasted measured SMB records can be explained by large-scale atmospheric circulation changes. We use historical snowfall and wind simulations as our initial state of the climate. The model prior

45 consists of a 10-member ensemble of SMB, 10-m winds (zonal and meridional surface winds) simulations downscaled from the Community Earth System Model version 2 (CESM2, Danabasoglu et al., 2020) down to the RACMO2.3 5.5km resolution (Lenaerts et al., 2017), using a statistical method described in Ghilain et al. (2022). This provides us with the best temporal and spatial distribution of SMB to understand the different time evolution of the local ice rises' SMB over the historical period. Our approach also allows us to understand the local SMB records better as we have a quantified estimate of the records'

50 uncertainties and a framework to test the role of those uncertainties compared to regional dynamics through the use of high spatial resolution downscaling and data assimilation.
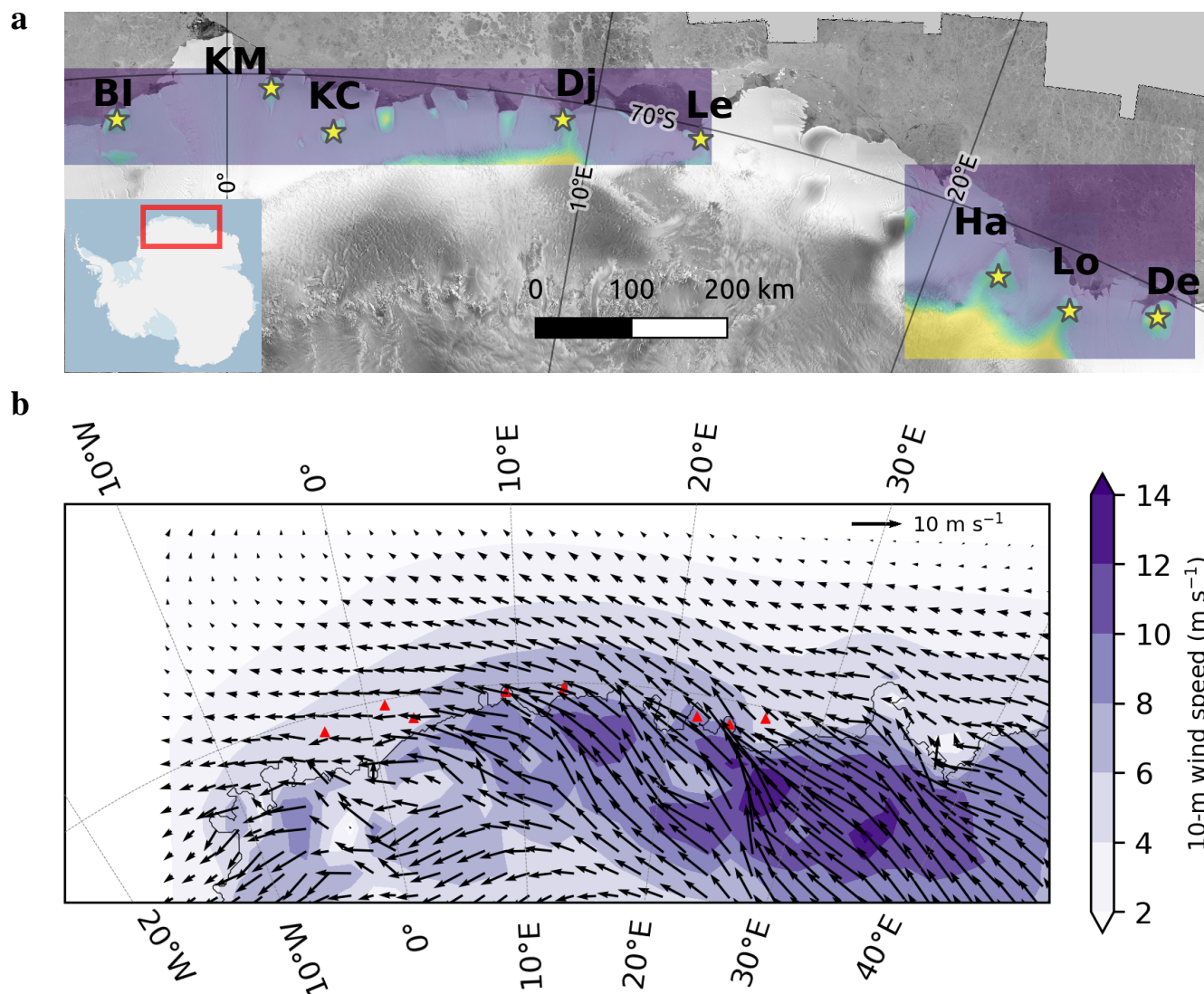
Figure 1. (a) Location of the eight ice cores along the Dronning Maud Land coast with the inset showing the Radarsat-1 Antarctic Mapping Project (RAMP) mosaic area. Site initials: BI is Blåskimen Island, KM is Kupol Moskovskij, KC is Kupol Ciolkovskogo, Dj is Djupranen, Le is Leningradkollen, Ha is Hammarryggen, Lo is Lokkeryggen and De is Derwael. Background is the RAMP RADARSAT mosaic (Jezek et al., 2013) with superimposed the Reference Elevation Model of Antarctica (REMA) v2 elevation for each site (units are meters and referenced to the WGS84 ellipsoid). This figure was prepared with Quantarctica (Matsuoka et al., 2021). (b) Mean 10-m winds over Dronning Maud Land for 1987-2011. Red triangles locate the ice core sites.

2 Methods

2.1 Data assimilation

The DA method implemented is identical to that described in a previous study (e.g. Dalaiden et al., 2021). We use an offline
approach and build the prior distribution, i.e. the initial state of the climate given by the model, from existing climate model
simulations (Steiger et al., 2017). The model simulations we choose are statistically downscaled snowfall simulations for
the period 1850-2014 (Ghilain et al., 2022). More info is provided in Section 2.3. The DA method is based on a particle
filter (Dubinkina et al., 2011). All the years (1850-2014) of our model simulations constitute the prior, and since we have
10 members, which arise from different internal variability, we start with 1650 particles. As the observations are annually
resolved, we apply an annual DA time step. The prior remains constant throughout the data assimilation process. Therefore,
the temporal variability in the reconstruction arises solely from the assimilated observations. During reconstruction, the prior
is directly compared with annual observations since the ice cores provide a direct measurement of SMB. Particle weights are
assigned based on the agreement between model results and observations, with closer matches receiving higher weights. The
mean reconstruction is determined by the weighted mean of the particles, while the range of the weighted ensemble provides
a measure of reconstruction uncertainty. Our observation error is the root-mean-square combination of the instrumental error
and the representativeness error (Supplementary Table S1). The instrumental error is calculated from the measurement error
propagated by the 1D inverse model applied to obtain the SMB records. We select the representativeness error estimated from
the difference between a point measurement at the ice core location and the mean radar-based estimate over a circle with a
radius of 3 km (as quantified in Cavitte et al. (2023)), which is a close match to the model prior with a spatial resolution of
5.5x5.5 km. We also augment this observation error by 10-50% to test the impact of potential uncertainty of this estimate of
the error on the reconstruction obtained (see Discussion).

2.2 SMB observations

We assimilate the ice core SMB records as anomalies (SMB record minus the temporal mean SMB over 1987-2011). We use
the published ice core SMB data for each of the eight ice rise core sites as described in Cavitte et al. (2023).

2.3 Downscaled model ensemble

The model ensemble is obtained through a statistical downscaling method which consists of associating snowfall simulations
from RACMO2.3p at the 5.5 km spatial resolution over Dronning Maud Land (Lenaerts et al., 2017) with specific weather
patterns from a coarser spatial resolution global climate model (ERA5, 0.25° in latitude-longitude), at a daily timescale. The
basis of the statistical downscaling is to evaluate the relationship between a high quality but shorter time frame reanalysis
dataset (here, ERA5, Hersbach et al., 2020) and a regionally optimized regional climate model simulation with a higher spa-
tial resolution (here, RACMO2.3p) to create an association database (Ghilain et al., 2022). The database associates the ten
main variability modes of four atmospheric fields providing information on large-scale circulation patterns (surface pressure,

geopotential height at 500 hPa, relative humidity at 700 hPa and precipitation) with the daily snowfall from RACMO2.3p. This database can be searched for analogs for periods not covered by RACMO2.3p or ERA5. The method is applied to the ensemble

85 members of the CESM2 Earth System Model (Danabasoglu et al., 2020) which has a lower spatial resolution but longer time frame to downscale the CESM2 results to the spatial scale of RACMO2.3p. This downscaled product has an improved spatio-temporal distribution of snowfall compared to global climate models, such as the CESM2 simulations on which it is based, and can thus provide information on large-scale atmospheric circulation patterns associated with local snowfall changes. In assimilating ice core SMB records with this downscaled snowfall dataset, we make the assumption that SMB and snowfall

90 are similar. In the framework of our methodology, this is a reasonable assumption for our region as CESM2 and RACMO2.3p obtain very similar results for snowfall and SMB.

Because we would like to reconstruct the large-scale atmospheric circulation linked to our SMB reconstructions, and this was not reconstructed in Ghilain et al. (2021), we apply the same method as used for snowfall to the wind components (zonal and meridional near-surface winds) of the CESM2 ensemble to obtain a 5.5 km resolved wind simulation ensemble. For this,

95 we use the time series of the 40 principal components obtained in the SMB downscaling as well as the principal components time series from ERA5 (Ghilain et al., 2021).

3 Results

Assimilating the eight ice core SMB records with the observation error quantified using the co-located radar datasets, we see that the reconstruction is able to reasonably fit the assimilated observations (Fig. 2a) with significant correlations (p-value $\leq$

100 0.05) between the reconstructed time series and the observed ice core time series for seven out of the eight ice core sites. The correlation values vary between 0.55 and 0.98 for all ice cores, except at KM which has a non-significant correlation of 0.28. The RMSE values between the observations and reconstruction remains below 10 cm w.e. yr^{-1} for six sites and up to 12 cm w.e. yr^{-1} for the other two. We also plot the RACMO2.3p SMB record extracted at the grid cell closest to the ice core sites but show that the reconstruction and the RACMO2.3p time series are statistically distinct, the correlation of the reconstruction

105 with RACMO2.3p being insignificant for a majority of the ice core sites and the RMSE higher than 10 cm w.e. yr^{-1} for most sites. However, we point out that the initial correlation of the ice core time series with the extracted RACMO2.3p time series is also weak. If we now examine the temporal correlation of the RACMO2.3p SMB simulation with the obtained reconstruction spatially (Fig. 2b), we observe a positive and significant correlation (p-value $\leq$ 0.05) for the eastern section of the DML coast, comprising the three easternmost ice rises assimilated (Ha, Lo and De), same for the western most section, including the three

110 western ice rises (BI, KM and KC) and a negative weaker correlation for the central section, although the ice core records show a strong positive correlation locally with RACMO2.3p. These SMB results show a good reconstruction from a technical standpoint, despite the heterogeneity of the ice core SMB records.

To understand how realistic our SMB reconstruction is from a physical standpoint, we must look at the associated large-scale atmospheric circulation that is reconstructed concomitantly using the 10-meter above-ground winds (Fig. 3 c-d). We look

115 at how the wind circulation has changed over the recent decade (2002-2011) with respect to the earliest decade reconstructed
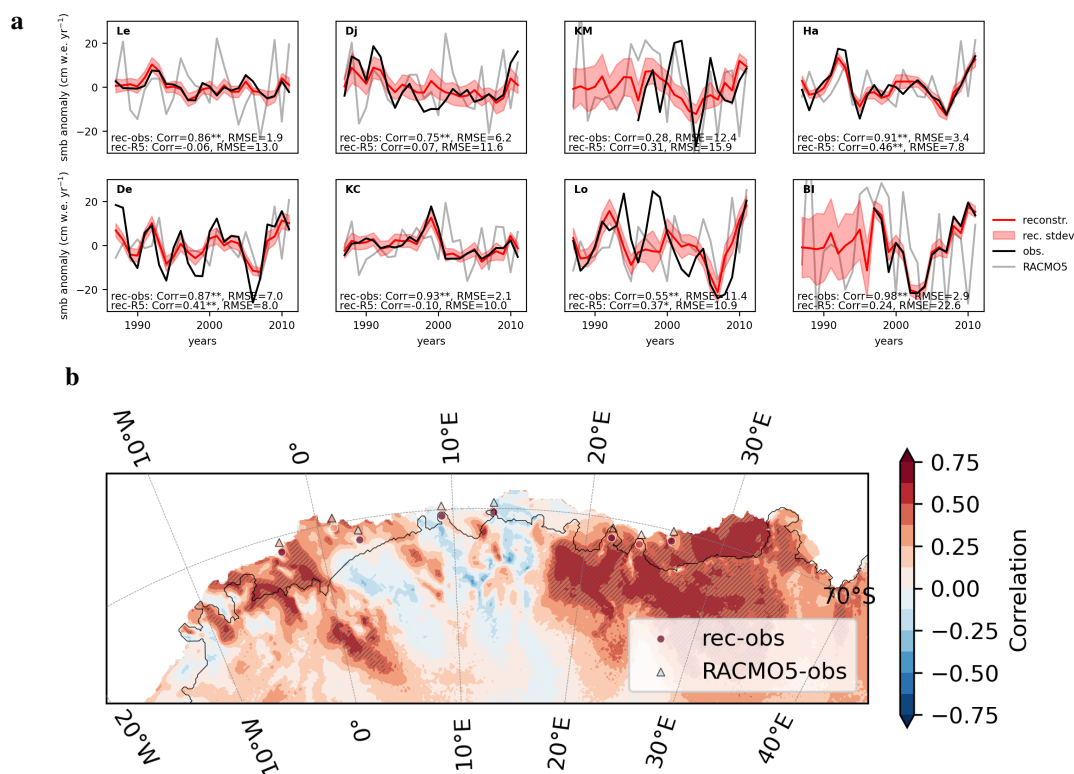
Figure 2. (a) SMB time series of the ice core records (black) versus ice-core based reconstruction (red) with reconstruction uncertainty in light red. Gray lines show the RACMO2.3p time series extracted at the ice core sites for comparison. Correlation and RMSE (in cm w.e. yr^{-1}) values are provided for each ice rise site, between the reconstruction ('rec') and the observations ('obs'), as well as the reconstruction and RACMO2.3p ('R5'). Correlations with a p-value ≤ 0.05 are double starred while a p-value of le 0.1 starred. (b) Spatial correlation between RACMO2.3p SMB and the SMB reconstruction. Hatchings highlight areas with a p-value ≤ 0.1; circles locate the ice core sites and are colored according to the value of the correlation between the ice core SMB and the reconstructed SMB locally; triangles are colored according to the value of the correlation between the observations and RACMO2.3p SMB locally (the triangles are offset vertically for ease of reading).

(1987-1996). This comparison is a test of the validity of the method used to reconstruct the winds, which will determine whether it can be applied over longer time intervals, when less direct measurements are available. We also contrast it to resulting SMB difference between those two periods (Fig. 3 a-b).

120 RACMO2.3p produces strong spatial contrasts in SMB (Fig.3b) and the same spatial patterns are observed in the reconstruction but with lower amplitudes (Fig. 3a). To obtain the best possible fit with the eight different SMB records which are located within hundreds of kilometers of each other, we notice that the large-scale atmospheric circulation is significantly modified (Fig. 3c) when comparing to RACMO2.3p (Fig. 3d), which we expect is relatively accurate at this spatial scale and decadal timescale (Agosta et al., 2019). Figure 3 shows the difference in wind strength between the youngest and oldest 10-year intervals of the reconstruction, so 2002-2011 versus 1987-1996. The reduction in decadal wind strength blowing from east to west
125 along the DML coast observed in RACMO2.3p is also observed in the reconstruction, particularly over western DML, but the difference is weaker from one decade to the next in the reconstruction. In eastern DML, the RACMO2.3p-observed increase in wind strength is not observed in the reconstruction. Furthermore, the ensemble reconstruction shows a stronger component of meridional flow over the ice rises, and over the DML coastline as a whole, than RACMO2.3p. The reconstruction is forced to create a lot of wind heterogeneity over the ice rises along the coastline to match the different local ice rises' signal at a
130 small spatial scale, but the spatial wind pattern obtained is not realistic and misses the large-scale patterns when compared to RACMO2.3p. We highlight that the number of particles retained by the filter is quite low (about 7% on average). Retaining too few particles implies that the reconstruction may be based on too few samples and the estimate may become less accurate (filter degeneracy). We have also tried applying an observation error augmented by 10%-50% to test the impact of a potential underestimation of the observation error, but this results in a worse match between the observations and the reconstruction, a
135 wind circulation mostly unchanged and does not significantly increase the number of particles kept within the DA framework (number of particles kept increases to 15% on average for an increase of 50% in the observation error).

4 Discussion and Perspectives

Assimilation of the ice core annual SMB records with a 5.5 km snowfall model ensemble can reconstruct the SMB field needed to reproduce the different ice core SMB time series with an observation error constrained from co-located radar measurements.
140 We confirm that for records where the calculated error is smaller, i.e. we have more trust in the SMB record, the accuracy of the reconstruction in reconstructing the measured SMB record is higher. However, the reconstructed wind anomalies resemble an over-fitting to observations in which changes in the synoptic circulation are trying to compensate for errors not well accounted for in our methodology, or processes at a smaller scale that the one resolved by RACMO2.3p.

Many other factors could be invoked to explain the contrasting ice core SMB records of the Dronning Maud Land coast. Ice
145 rises are generally small (tens of kilometers in width), yet with a strong topographic gradient (hundreds of meters in height above sea level). De ice rise for example is a thick dome-shaped ice rise entirely located within the Roi Baudouin Ice Shelf and reaches a maximum height of 429 m above sea level, with a maximum ice thickness of 550 m for a 31-km width east-west and 40 km north-south (Cavitte et al., 2022). Because of their topography, ice rises are influenced by various local scale
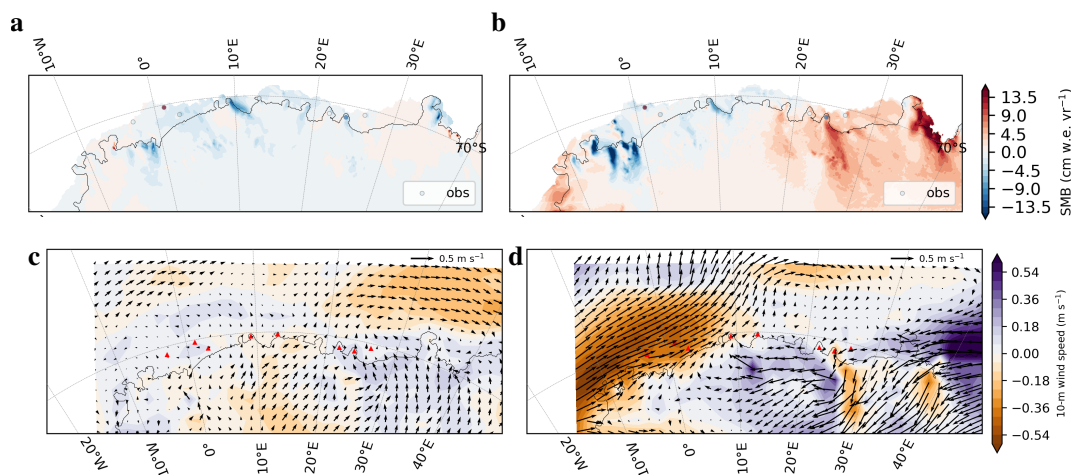
Figure 3. Difference in (a-b) SMB and (c-d) wind circulation between youngest and oldest 10-year intervals of the reconstruction (namely, variable temporal mean over 2002-2011 minus average over 1987-1996). Left column shows the results for the reconstruction (a and c), right column shows the results for RACMO2.3p (b and d). Circles in panels a and b show the difference in SMB for the ice core data; red triangles in panels c and d locate the ice core sites. Note that the region shown in panels a-b is zoomed in onto the grounded ice sheet as opposed to c-d which show atmospheric circulation offshore.

effects which act at a smaller scale than the RACMO2.3p grid size. Kausch et al. (2020) have shown that ice rises' SMB
150   records are strongly affected by wind-driven redistribution of snow at the ice crest. In addition, we note the wide range of
shapes of the ice rises, with some connected to the main land, and others entirely surrounded by ice shelves. Interactions of
the synoptic circulation coming from the Southern Ocean with the katabatic winds from the ice sheet interior could affect
snow redistribution. The contrasting ice rise geometries combined with the local wind influence could significantly locally
modify a large-scale SMB signal. These local effects will therefore modify the SMB time series recorded by the ice cores
155   during or after snowfall events. In addition, ice flow dynamics within the ice rises could have changed the position of the ice
crest maximum over time, however this should not have a large impact on a few decades. Another potential reason for the
disagreement between the reconstruction and observed/modeled atmospheric circulation is that we use a downscaled model
ensemble based on snowfall associations in which we assimilate ice core SMB records. So if surface snow redistribution plays
a large role in the individual ice cores' SMB records, this is not captured in the model ensemble. However, RACMO2.3p SMB
160   does not reproduce well the small-scale process such as those linked with wind redistribution (Agosta et al., 2019) and therefore
a downscaled SMB model ensemble would not have significantly changed the results in this case. We repeated the DA using
the radar-derived SMB (which retains the ice core's temporal variability, as shown in Cavitte et al. (2023)) directly with its
associated observation errors and the same model prior (Supplement S2). The SMB and wind spatial patterns obtained are
distinctly different from the ice core-based reconstruction's and from the patterns observed in RACMO2.3p. This radar-based
165   reconstruction is technically sound with the hypotheses chosen but the results are not robust, over-fitting of the radar data inputs
is observed once again. The reconstruction obtained is sensitive to the assimilated data.

Münch et al. (2017) show that an ice core is not necessarily representative of a very wide surface area. A combination of both sub-annual and local spatial processes might be at work to explain the different SMB records observed on the ice rises. A solution could be to average several ice cores. However, this is difficult to do with the limited number of ice cores available. Another option would be to assimilate the ice core records at a lower temporal resolution to increase the signal-to-noise in the records. The reconstruction is particularly difficult due to the complexity of the region, with very contrasted topography and therefore potentially strong wind interactions with the relief. Perhaps attempting a similar reconstruction but applied to a region with smoother topographic relief could improve the skill of the reconstruction. We note that the ice core SMB records used here are uncorrected for vertical strain rates. But as we only examine the top 50 m of the ice column, we can reasonably assume that this has a minimal impact on the SMB reconstructed over the corresponding time period. We also note that although RACMO2.3p captures well large-scale atmospheric circulation, being constrained by ERA-Interim reanalysis (Lenaerts et al., 2017), this model has large errors in SMB locally, especially in topographically complex areas such as the DML coastline (Kausch et al., 2020; Cavitte et al., 2020).

5 Conclusions

By combining a high resolution downscaled atmospheric circulation model ensemble and well constrained ice core SMB records from quantified observation errors using co-located radar observations through a DA framework, we are able to reconstruct well the annual ice core SMB records measured at eight ice rises along the DML coast. However, although the DA experiments work from a technical standpoint, the large-scale atmospheric circulation reconstructed patterns do not agree with the regional climate model RACMO2.3p for the region. We conclude that annual large-scale circulation changes only cannot explain the observed local records of SMB. A combination of local effects at a smaller spatial scale than 5.5 km and precipitation events at the sub-annual timescale might be able to explain the contrasting ice core records. Because the ice core records are rarely sub-annually resolved, due to the nature of the measurements (if we want to go back further than 10 years), we would need to turn to other types of SMB records such as automatic weather stations. The issue in that case is that such records are currently not long enough to retrieve meaningful SMB trends. Although the radar-derived SMB provide local constraints on the error of representativeness of the SMB records, they potentially still underestimate the full uncertainties of the records. On the other hand, as regional climate models improve in grid resolution with increasing computer power and the emergence of ML and AI emulators, very high resolution regional climate or snow models might soon provide appropriate simulations to examine the contribution of local wind circulation in local SMB measurements.

Code and data availability. Radar-derived SMB can be found at https://doi.org/10.14428/DVN/J34MQO (Cavitte, 2023). RACMO2.3p simulations are available by request to J. M. (Melchior) van Wessem (j.m.vanwessem@uu.nl). Downscaled annual snowfall, the PCs and the EOFs used for the downscaling are available at https://doi.org/10.5281/zenodo.4287517 (Ghilain et al., 2021); downscaled annual wind simulations are available at xxxx.

Author contributions. MGPC led the data analysis, assimilation, wind-downscaling and writing. HG provided rich discussions in planning the experiments. QD provided the data assimilation framework and support for running the experiments. NG provided the downscaling expertise. All co-authors contributed to the discussions on this work. MGPC prepared the paper with contributions from all co-authors.

Competing interests. The authors declare that they have no competing interests.

Acknowledgements. We would like to thank all those involved in data collection, ice core and radar data processing under the Mass2Ant and MADICE projects upon which this study relies. Marie Cavitte and Quentin Dalaiden were postdoctoral researchers of the FRS-FNRS for the duration of the study. Hugues Goosse is a research director within the FRS-FNRS. Nicolas Ghilain is funded by the Belgian Science Policy through the Fed-tWin program

References

Agosta, C., Amory, C., Kittel, C., Orsi, A., Favier, V., Gallée, H., van den Broeke, M. R., Lenaerts, J., van Wessem, J. M., van de Berg, W. J., et al.: Estimation of the Antarctic surface mass balance using the regional climate model MAR (1979-2015) and identification of dominant processes, Cryosphere, 13, 281–296, 2019.

210 Casado, M., Münch, T., and Laepple, T.: Climatic information archived in ice cores: impact of intermittency and diffusion on the recorded isotopic signal in Antarctica, Climate of the Past, 16, 1581–1598, https://doi.org/10.5194/cp-16-1581-2020, 2020.

Cavitte, M.: Gridded surface mass balance derived from shallow radar stratigraphy over eight ice rises along the Dronning Maud Land coast and one site in the Dome Fuji region, Antarctica, https://doi.org/10.14428/DVN/J34MQO, 2023.

Cavitte, M. G., Goosse, H., Wauthy, S., Kausch, T., Tison, J.-L., Van Liefferinge, B., Pattyn, F., Lenaerts, J. T., and Claeys, P.: From ice core

215 to ground-penetrating radar: representativeness of SMB at three ice rises along the Princess Ragnhild Coast, East Antarctica, Journal of Glaciology, 68, 1221–1233, https://doi.org/10.1017/jog.2022.39, 2022.

Cavitte, M. G. P., Dalaiden, Q., Goosse, H., Lenaerts, J. T. M., and Thomas, E. R.: Reconciling the surface temperature–surface mass balance relationship in models and ice cores in Antarctica over the last 2 centuries, The Cryosphere, 14, 4083–4102, https://doi.org/10.5194/tc-14-4083-2020, 2020.

220 Cavitte, M. G. P., Goosse, H., Matsuoka, K., Wauthy, S., Goel, V., Dey, R., Pratap, B., Van Liefferinge, B., Meloth, T., and Tison, J.-L.: Investigating the spatial representativeness of East Antarctic ice cores: a comparison of ice core and radar-derived surface mass balance over coastal ice rises and Dome Fuji, The Cryosphere, 17, 4779–4795, https://doi.org/10.5194/tc-17-4779-2023, 2023.

Dalaiden, Q., Goosse, H., Rezsohazy, J., and Thomas, E. R.: Reconstructing atmospheric circulation and sea-ice extent in the West Antarctic over the past 200 years using data assimilation, Climate Dynamics, pp. 3479–3503, https://doi.org/10.1007/s00382-021-05879-6, 2021.

225 Danabasoglu, G., Lamarque, J.-F., Bacmeister, J., Bailey, D. A., DuVivier, A. K., Edwards, J., Emmons, L. K., Fasullo, J., Garcia, R., Gettelman, A., Hannay, C., Holland, M. M., Large, W. G., Lauritzen, P. H., Lawrence, D. M., Lenaerts, J. T. M., Lindsay, K., Lipscomb, W. H., Mills, M. J., Neale, R., Oleson, K. W., Otto-Bliesner, B., Phillips, A. S., Sacks, W., Tilmes, S., van Kampenhout, L., Vertenstein, M., Bertini, A., Dennis, J., Deser, C., Fischer, C., Fox-Kemper, B., Kay, J. E., Kinnison, D., Kushner, P. J., Larson, V. E., Long, M. C., Mickelson, S., Moore, J. K., Nienhouse, E., Polvani, L., Rasch, P. J., and Strand, W. G.: The Community Earth System Model Version 2

230 (CESM2), Journal of Advances in Modeling Earth Systems, 12, e2019MS001 916, https://doi.org/https://doi.org/10.1029/2019MS001916, e2019MS001916 2019MS001916, 2020.

Dubinkina, S., Goosse, H., Sallaz-Damaz, Y., Crespin, E., and Crucifix, M.: Testing a particle filter to reconstruct climate changes over the past centures, International Journal of Bifurcation and Chaos, 21, 3611–3618, https://doi.org/10.1142/S0218127411030763, 2011.

Ghilain, N., Vannitsem, S., Dalaiden, Q., Goosse, H., and De Cruz, L.: MASS2ANT Snowfall Dataset (Downscaling @5.5km over Dronning

235 Maud Land, Antarctica, 1850 - 2014), https://doi.org/10.5281/zenodo.4287517, 2021.

Ghilain, N., Vannitsem, S., Dalaiden, Q., Goosse, H., De Cruz, L., and Wei, W.: Large ensemble of downscaled historical daily snowfall from an earth system model to 5.5 km resolution over Dronning Maud Land, Antarctica, Earth System Science Data, 14, 1901–1916, https://doi.org/10.5194/essd-14-1901-2022, 2022.

Hersbach, H., Bell, B., Berrisford, P., Hirahara, S., Horányi, A., Muñoz-Sabater, J., Nicolas, J., Peubey, C., Radu, R., Schepers, D., Sim-

240 mons, A., Soci, C., Abdalla, S., Abellan, X., Balsamo, G., Bechtold, P., Biavati, G., Bidlot, J., Bonavita, M., De Chiara, G., Dahlgren, P., Dee, D., Diamantakis, M., Dragani, R., Flemming, J., Forbes, R., Fuentes, M., Geer, A., Haimberger, L., Healy, S., Hogan, R. J., Hólm, E., Janisková, M., Keeley, S., Laloyaux, P., Lopez, P., Lupu, C., Radnoti, G., de Rosnay, P., Rozum, I., Vamborg, F., Vil-

laume, S., and Thépaut, J.-N.: The ERA5 global reanalysis, Quarterly Journal of the Royal Meteorological Society, 146, 1999–2049, https://doi.org/https://doi.org/10.1002/qj.3803, 2020.

245   Hirsch, N., Zuhr, A., Münch, T., Hörhold, M., Freitag, J., Dallmayr, R., and Laepple, T.: Stratigraphic noise and its potential drivers across the plateau of Dronning Maud Land, East Antarctica, The Cryosphere, 17, 4207–4221, https://doi.org/10.5194/tc-17-4207-2023, 2023.

Jezek, K. C., Curlander, J. C., Carsey, F., Wales, C., and Barry, R. G.: RAMP AMM-1 SAR Image Mosaic of Antarctica, 2013.

Kausch, T., Lhermitte, S., Lenaerts, J. T. M., Wever, N., Inoue, M., Pattyn, F., Sun, S., Wauthy, S., Tison, J.-L., and van de Berg, W. J.: Impact of coastal East Antarctic ice rises on surface mass balance: insights from observations and modeling, The Cryosphere, 14, 3367–3380,

250   https://doi.org/10.5194/tc-14-3367-2020, 2020.

Lenaerts, J., Lhermitte, S., Drews, R., Ligtenberg, S., Berger, S., Helm, V., Smeets, C., Van den Broeke, M., Van De Berg, W. J., Van Meijgaard, E., et al.: Meltwater produced by wind–albedo interaction stored in an East Antarctic ice shelf, Nature climate change, 7, 58, 2017.

Lenaerts, J. T. M., Medley, B., van den Broeke, M. R., and Wouters, B.: Observing and Modeling Ice Sheet Surface Mass Balance, Reviews

255   of Geophysics, 57, 376–420, https://doi.org/10.1029/2018RG000622, 2019.

Medley, B. and Thomas, E.: Increased snowfall over the Antarctic Ice Sheet mitigated twentieth-century sea-level rise, Nature Climate Change, 9, 34, 2019.

Münch, T., Kipfstuhl, S., Freitag, J., Meyer, H., and Laepple, T.: Constraints on post-depositional isotope modifications in East Antarctic firn from analysing temporal changes of isotope profiles, The Cryosphere, 11, 2175–2188, https://doi.org/10.5194/tc-11-2175-2017, 2017.

260   Steiger, N. J., Steig, E. J., Dee, S. G., Roe, G. H., and Hakim, G. J.: Climate reconstruction using data assimilation of water isotope ratios from ice cores, Journal of Geophysical Research: Atmospheres, 122, 1545–1568, 2017.

Valler, V., Brugnara, Y., Franke, J., and Brönnimann, S.: Assimilating monthly precipitation data in a paleoclimate data assimilation framework, Climate of the Past, 16, 1309–1323, https://doi.org/10.5194/cp-16-1309-2020, 2020.

Van Wessem, J. M., Jan Van De Berg, W., Noël, B. P., Van Meijgaard, E., Amory, C., Birnbaum, G., Jakobs, C. L., Krüger, K., Lenaerts, J.,

265   Lhermitte, S., et al.: Modelling the climate and surface mass balance of polar ice sheets using RACMO2: Part 2: Antarctica (1979-2016), The Cryosphere, 12, 1479–1498, 2018.

Wang, Y., Ding, M., Reijmer, C. H., Smeets, P. C. J. P., Hou, S., and Xiao, C.: The AntSMB dataset: a comprehensive compilation of surface mass balance field observations over the Antarctic Ice Sheet, Earth System Science Data, 13, 3057–3074, https://doi.org/10.5194/essd-13-3057-2021, 2021.